Surface Science 54 (1976) 419–433

SURFACE CRYSTALLOGRAPHY OF THE c(2X2) SODIUM OVERLAYER ON Al(100)*

B.A. HUTCHINS and T.N. RHODIN
School of Applied and Engineering Physics, Cornell University, Ithaca, New York 14853, U.S.A.

and

J.E. DEMUTH
IBM Thomas J. Watson Research Center, Yorktown Heights, New York 10598, U.S.A.

Received 19 August 1975

Experimental LEED intensity–energy spectra are reported for clean Al(100) and for c(2×2)Na on Al(100). The experimental results are compared with spectra calculated with the layer–KKR method and found to be in good agreement for both the clean surface and the overlayer. For the overlayer, the best agreement is obtained for Na atoms in the four-fold hollow site at a perpendicular distance of 2.05 ± 0.1 Å.

1. Introduction

Analysis of the diffraction intensities of LEED measurements can be used to determine the atomic positions of various adsorbates on single crystal surfaces [1–5]. From Porteus' work on Na overlayers in Al(100) [6], it is known that a c(2X2) overlayer exists. In this work we have obtained experimental LEED spectra for the clean Al(100) surface and for an ordered c(2X2) overlayer of Na on Al(100) and have compared them to calculated LEED spectra in an effort to determine the location of adsorbed Na on Al(100). Such crystallographic information for Na on Al may not only provide a useful test for realistic quantum mechanical calculations of a free-electron-like chemisorption system but can also be compared to the case of Na on Ni(001) [7,8] to provide insight as to possible chemical differences between chemisorption on a transition metal versus a free electron metal.

* Supported by National Science Foundation and by ARPA through Cornell MSC.

2. Experimental procedures

Al(100) surfaces were prepared by mechanical polishing with alumina abrasive starting with 1 μm size and finishing with 0.3 μm size. Polishing with finer abrasive was found to produce an undulating rather than a smooth flat surface. Shiny surfaces free of mechanical damage due to polishing were produced by electropolishing [9] with a current density of 5 A/cm^2. A UHV sample manipulator and LEED system developed in an earlier study by Ignatiev, Jones and Rhodin [10] were adapted for the present study. The system permitted the study of surfaces for polar angles from zero to 22° (accurate to ±1°), beam energies from 30 to 1000 V, and temperatures from 110 K (with liquid nitrogen cooling) to 300 K. Intensity versus energy plots of diffraction spots were obtained with a spot photometer and normalized electronically [11]. Absolute reflectivities were calibrated by measuring the incident and diffracted spot intensities with a Faraday collector but were not used in the analysis. A diagram of the experimental setup is shown in fig. 1.

In this work a Na vapor source was used to form the overlayer instead of the Na-zeolite source as used by Porteus [6]. Sodium metal sealed in a Pyrex ampoule was introduced into the LEED system prior to bakeout. After a base pressure of 1×10^{-10} torr was obtained, the Al(100) surface was cleaned by xenon ion bombardment and extended periods of anneal at 850 K. The cleaning process was monitored with Auger electron spectroscopy using the LEED optics as an energy analyzer. The Al surface was judged to be clean and ready for examination when a satisfactory LEED pattern was produced and a 25:1 ratio was obtained between the amplitudes of the 67 V and 53 V peaks in the AES spectrum [12].

The spectrum noise level in the AES spectra relative to the aluminum signal intensity correspond to a sensitivity of about 1% of a monolayer for oxygen. Contaminant levels on the sodium layers used for measurement were difficult to determine. The chief contaminant, oxygen, was estimated on the average to be less than 5% and judged to be distributed on the surface so as not to interfere with the measurements. Exploratory studies prior to the main measurements indicated no significant effects of the electron beam on the heterogeneous decomposition of CO or on the desorption of sodium from the surface. Both ion sputtering heating and thermal desorption were useful in cleaning the surface before each new sodium deposition. The latter was remarkably effective in removing the sodium and restoring the clean surface. Cleaning by ion-bombardment was more effective, especially when it was required to remove surface constituents other than sodium. Both methods were compared and evaluated.

After clean Al(100) surfaces were obtained and examined the Na-metal source was prepared for use. A nickel ribbon filament around the glass ampoule was outgassed by a series of short flashes to 1000 K. Next a lever arrangement was used to break off the tip of the ampoule along a line previously determined by scoring the glass with a file before insertion into the UHV system. The ampoule had been sealed under high vacuum and produced a slight pressure burst when the tip was broken (of no consequence). A high density flux of Na metal was then produced by heating

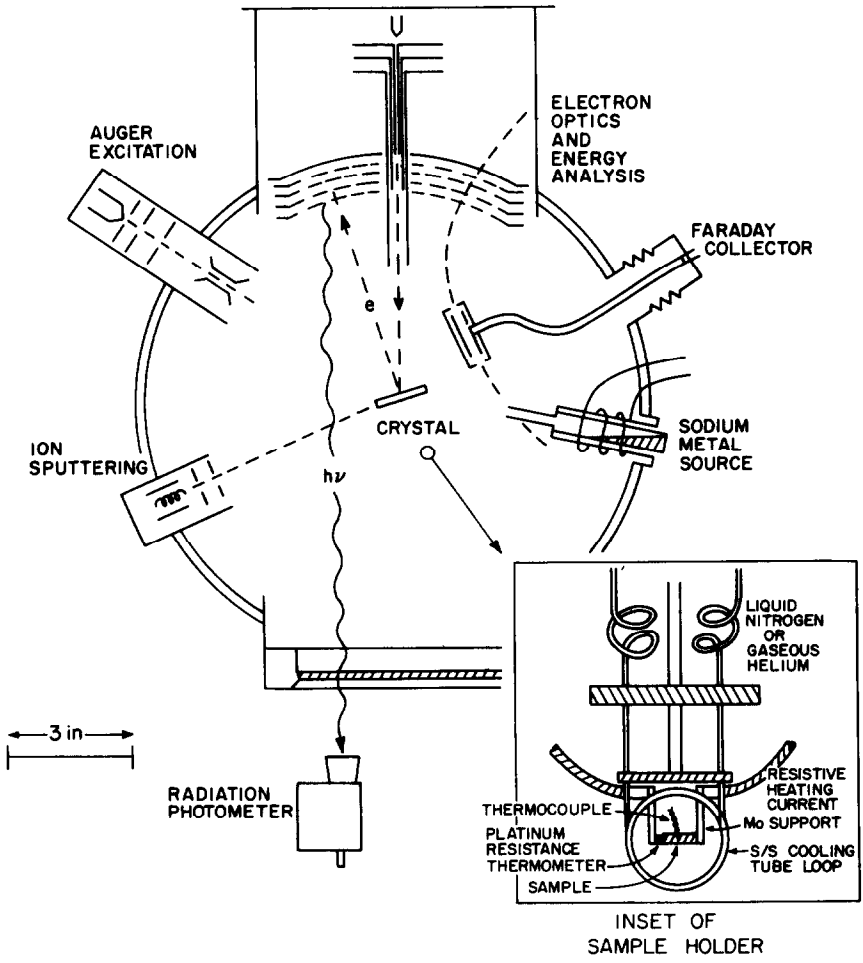

Fig. 1. Diagramatic sketch of the ultra high vacuum LEED/Auger spectrometer showing the sample cooling manipulator, Na-metal vapor source, Faraday collector and spot photmeter used in these measurements.

the Ni ribbon filament to 900 K [13]. A stainless steel shield was placed in front of the LEED optics during exposure of the sample to prevent contamination which would change the work function of the grids. During exposure the sample was maintained at 250 K by liquid nitrogen cooling. The titanium sublimator of the vacuum system was cooled with liquid nitrogen to keep the pressure in the low 10^{-10} torr range. After an exposure of about 5 min, the Al substrate was heated to 360 K to anneal the Na overlayer. Without annealing, only a diffuse LEED pattern is observed. Typically, three exposures and anneals were required to produce an ordered c(2X2)

structure. The c(2×2) structure was determined by the appearance of the proper LEED pattern and by measurement of the change of the surface work function. These work function changes were measured using the LEED system [14] and the value obtained (−1.45 eV) agreed to within 5% of the value obtained by Porteus [6] for a half-monolayer coverage. (Since Porteus used a zeolite ion source, he was thus able to determine coverages accurately by measuring current.) In the present study, a Na-metal source was chosen so as to avoid any complications due to possible chlorine or oxygen contamination from the zeolite source.

Measurements of the LEED spectra were taken below room temperature by maintaining liquid nitrogen cooling. The lowered temperatures provided a much higher spot intensity. Although the cooled substrate is subject to a faster rate of contamination, it was found that as long as the titanium sublimator was cooled, cooling was a benefit. In the actual experimental procedure, measurements were first made on the Al/Na system, the Na was removed by heating, and the corresponding clean Al measurements were made. This avoided problems associated with the resetting of the polar angle, as the manipulator was not moved between the two sets of measurements. This procedure does not, however, produce the best quality data for the clean Al surface since cleaning by heating alone is not as effective as ion sputtering and heating. Therefore, some corrections were made in the low energy features so that they correspond to the better clean Al data obtained before the study of the overlayer was undertaken.

3. Theoretical calculations

The intensity spectra were calculated using the layer KKR (Korringa–Kohn–Rostoker) method [15]. The model parameters were chosen so as to permit best agreement with experiment. The scattering potentials for both Al and Na were obtained from self-consistent band structure calculations [17] which included exchange-correlation via a local-density contribution, as suggested by Hedin–Lundqvist [18]. Although "simple" Al superposition potentials are known to provide nearly identical LEED spectra as a self-consistent potential [16], these former potentials do not usually provide a well-defined Fermi level with respect to their muffin-tin zeros while the latter do – thereby enabling us to select a "static" inner potential based upon the established work function of the surface. The inner potential for clean Al was thus set to a static value of 8.2 + 3.9 = 12.1 eV [19]. For the case of Na on Al(001) the (negative) change in work function was added to this value and the Fermi levels of the Na and Al potentials were set equal. Setting Fermi levels equal displaces the muffin-tin zeros of the two potentials, producing a discontinuity. We thus impose a no reflection condition at this boundary. For the overlayer case, the reflection and transmission of propagating waves into and out of surface (i.e. surface barrier) was also included. Such prescriptions for matching the adsorbate and substrate potentials and for accounting for the surface has been shown to pro-

vide best agreement between theory and experiment at low energies ($\lesssim 50$ eV) for Na on Ni(001) [8]. Since intensity calculations for the $(\frac{1}{2}\,\frac{1}{2})$ beam were needed down to about 30 eV these latter considerations were necessary.

Fortunately here, as in the case of Na/Ni(001), the resulting work function for the c(2×2) structure is close to the work function of metallic Na – and suggests that little charge transfer occurs. In the case of Na/Ni(001) [8] charge transfer was found from an SCF X-α cluster calculation of $NaNi_4$ to be negligibly small. Moreover, the resulting Na potential provided LEED spectra identical to those obtained with the metallic potential. Thus, we believe a metallic Na absorbate potential should also be suitable here. For clean Al, calculations were also made using Snow's self-consistent potential [20] and were found to yield LEED spectra indistinguishable from our potential, and therefore are not discussed. (The use of a different inner potential with Snow's Al potential in earlier calculations [15,16] will be briefly commented on in the next section.)

Thermal scattering was added to the model through the use of two effective Debye temperatures. For clean Al-metal, a bulk Debye temperature of 339 K was used [15] and a smaller Debye temperature for the surface Al atoms (due to increased surface vibrations) was determined from the temperature dependence of the intensities. Comparison of the calculated spectra (for a range of surface Debye temperatures) to the experimental peaks near 30 eV and 130 eV in the 00 beam at $\theta = 4.4°$ for 110, 300 and 540 K provided a reasonable fit for $\theta_D^s = 170$ K. This value is in agreement with that determined by Laramore [21] based on other experimental data [22]. For the overlayer case we have assumed the same force constants as for Al surface atoms on the clean surface scale θ_D to account for the mass difference (all underlying Al atoms retain a bulk θ_D). This gives a θ_D^s for Na of ~150 K. Although this represents a gross approximation, variations in θ_D by ±100 K, in these calculations generally affect the intensities but not the overall spectral features in the LEED profiles.

Two choices of an energy-independent imaginary potential (used to represent inelastic processes) of 5.5 eV and 3.4 eV were examined. The former was chosen from the higher energy region (~100 eV) of the free electron gas self-energy calculations [23], while the latter value is approximately the value used in previous calculations [15]. Use of the smaller damping parameter resulted in too much fine structure (particularly at energies above 100 eV) which was not apparent in the logarithmic data. The larger damping produced fine structure more comparable to experiment and was therefore used. The imaginary potential used in the Na overlayer was chosen to be 3 eV. Adjustments in this parameter did not produce the noticeable modifications in the calculated spectra as observed for clean Al:

In calculating the intensity spectra, 8 phase shifts were used to describe both the Na and Al scattering potentials with 39 beams considered for clean Al and 29 and 58 beams considered for the substrate and overlayer respectively. The intensities were calculated every 1.5 eV up to 100 eV and every 2.0 eV from 100 eV to 240 eV, machine plotted and hand-smoothed to yield the "calculated" spectra.

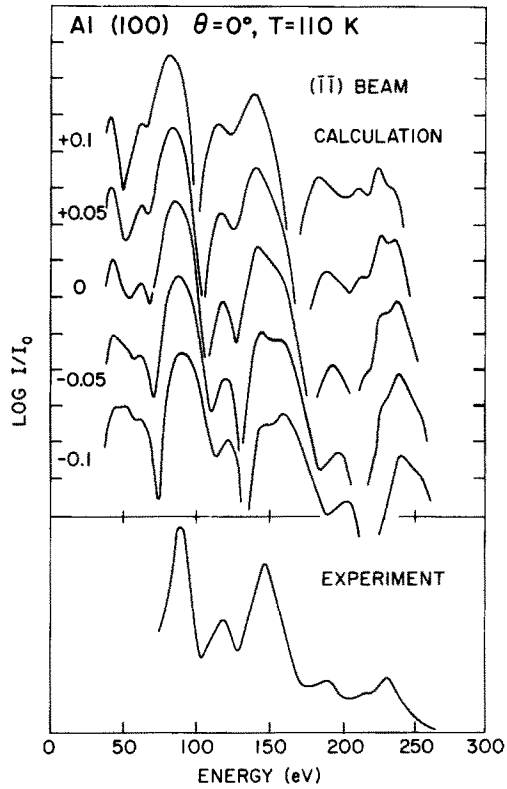

Fig. 2. Comparison of the $(\bar{1}\bar{1})$ beam experimental results for the Al(100) surface with calculations for expansions and contraction of the first surface layer by 0.1 and 0.05 Å. The experimental scale has been shifted by −6 eV.

4. Comparison of theory to experiment

In order to check the model as well as to establish the model parameters, calculations were first made for clean Al(001) for $T = 110$ K. Theoretical and experimental results were compared for the (00) beam at polar angles of 4.4°, 7°, 12° and for the $(\bar{1}0)$ and $(\bar{1}\bar{1})$ beams at normal incidence. In comparing these results two adjustments were found to be necessary to provide proper agreement. The first adjustment consisted of considering only relative diffraction intensities, since the absolute reflectivities of the calculated spectra were about five times larger than those measured. Since the experimental energy scale in these experiments is not referenced, we have chosen to use the "static" value of the inner potential in the calculation and to shift the experimental energy scale to align peak positions. Thus, the second adjustment consisted of shifting the experimental energy scale by 6 eV to lower energy for clean Al so as

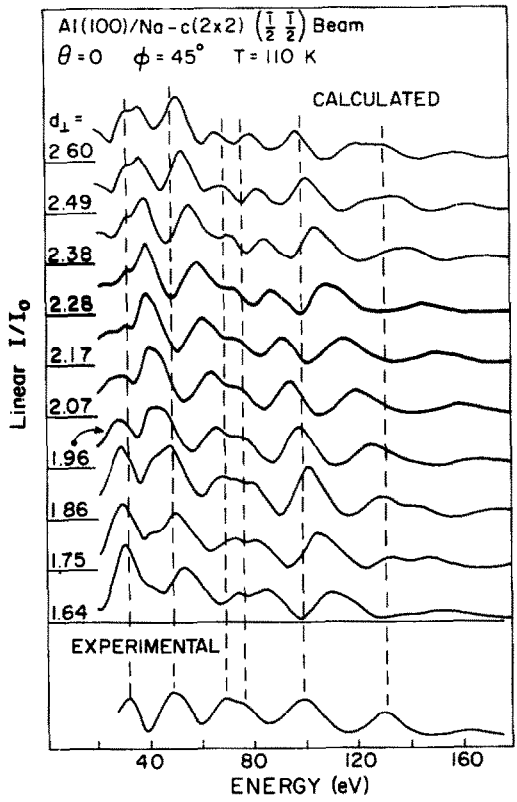

Fig. 3. Comparison of the $(\bar{\frac{1}{2}}\,\bar{\frac{1}{2}})$ beam experimental results ($\theta = 0°$), for Al(100)/Na–c(2×2) with calculated spectra for Na in the four-fold hollows at distances between 2.6 to 1.64 Å. The experimental scale has been shifted by −6 eV.

to match peak positions between 150 to 200 eV. (This 6 eV shift was also used for the overlayer comparisons.) Part of this shift can be atributed to contact potential differences and offset voltages in the electron optics and sweep circuits. Although the absolute values of the experimental corrections are uncertain, they are energy independent, hence this procedure should determine the *deviation* from our static inner potential as a function of energy. This will be discussed later.

After making these adjustments good agreement is achieved between calculated and experimental spectra for the unrelaxed surface. Comparisons were also made with the first Al layer compressed and expanded by 0.05 Å and 0.1 Å. Such a comparison is shown for the $(\bar{1}\,\bar{1})$ beam at normal incidence in fig. 2. (Note that the use of logarithmic scales accentuates many details of the spectra not observable with linear scales.) As in previous work [15] there is no indication here or for the other beams or incident angles, that either the relaxed or contracted clean surfaces agree

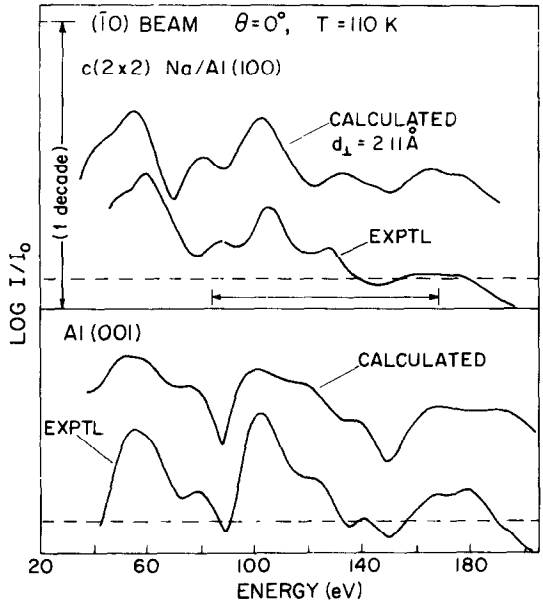

Fig. 4. Comparison of the $(\bar{1}0)$ beam experimental results ($\theta = 0°$) for clean Al(100) and Al(100)/Na–c(2X2) with calculated spectra. For the overlayer Na sits in the four-fold hollow. The experimental energy scale has been shifted by −6 eV.

more favorably than the undistorted surface.

For the case of the c(2X2) Na overlayer calculations the substrate was assumed undistorted and the absorbate site and perpendicular displacement normal to the surface was varied. Calculations were made for one, two and four-fold (hollow) sites for 0.1 Å differences in perpendicular displacements so as to cover a range between 1.4 Å to 3.4 Å (site dependent range). The best agreement between theory and experiment for all beams and angles considered occurred for the four-fold hollow site. In fig. 3 is shown a comaprison of the calculated spectra to the experiemtnal spectra for the $(\frac{1}{2}\,\frac{1}{2})$ beam at normal incidence. The best agreement in terms of matching the overall lineshapes and relative peak positions occurs for the 1.9 Å displacement. In examining the integral order beams at normal incidence the best agreement again in terms of matching spectral lineshapes and relative peak position occurs for $d_\perp$ = 2.11 Å. The comparison is shown in fig. 4 for the $(\bar{1}0)$ beam and in fig. 5 for the $(\bar{1}\bar{1})$ beam. Also shown for comparison are the clean surface results for these beams. The spectral features in the integral order beams which are changed upon adsorption are indicated by the horizontal arrows below the overlayers spectra. It is to these regions that we pay particular attention in our analysis of the integral order beams. In figs. 6 and 7 we similarly compare the (00) beam for $\theta = 7°$ and 12° along $\phi = 45°$. Again we show both clean and overlayer comparisons where for the overlayer case best

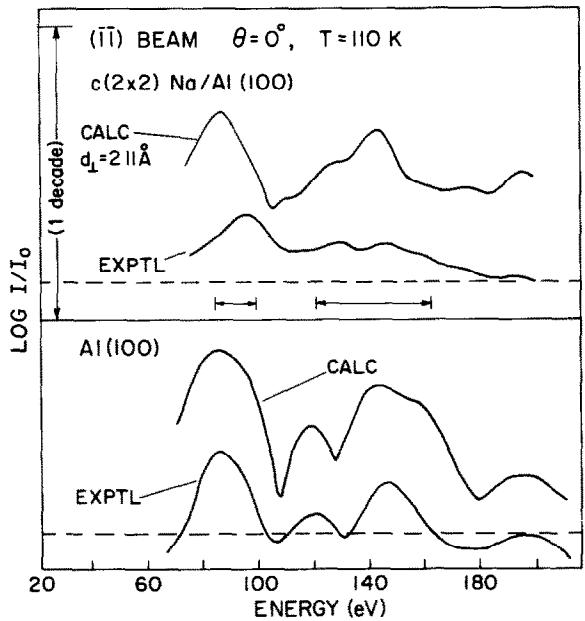

Fig. 5. Comparison of the $(\bar{1}\bar{1})$ beam experimental results ($\theta = 0°$) for clean Al(100) with calculated spectra and Al(100)/Na–c(2×2). For the overlayer Na sits in the four-fold hollows. The experimental energy scale has been shifted by −6 eV.

agreement is obtained for $d_\perp = 2.07$ Å. Weighting the integral beam normal incidence, off normal incidence and fractional order beam results equally we obtain a $d_\perp$ for Na on Al(001) of 2.05 ± 0.1 Å (where all beams considered provide optimal agreement within this range of displacement).

5. Discussion

5.1. Experimental and calculated spectra

In comparing this data with the earlier data obtained by Jona [9] we find that relatively good agreement exists between the two sets of data. The peak positions in both experiments agree within ±3 eV, even though neither has a well-defined reference level for the energy scale. Thus, the agreement between theory and experiment achieved here for clean Al is comparable to that obtained earlier [15,16]. (The previous calculations with the layer–KKR method were not carried to as high an energy and used fewer beams.) Although detailed comparisons of peak positions were not made in these earlier works it is instructive to consider them here. The calculations here with a "static" inner potential of 12 eV and a −6 eV shift in the experi-

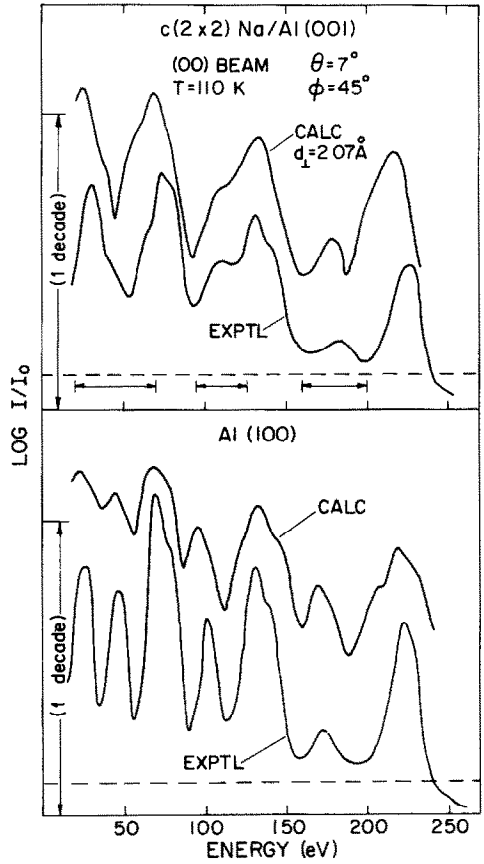

Fig. 6. Comparison of the (00) beam experimental results ($\theta = 7°$, $\phi = 45°$) for clean Al(100) with calculated spectra and Al(100)/Na–c(2×2). For the overlayer Na sits in the four-fold hollows. The experimental energy scale has been shifted by −6 eV. (Azimuthal angle of 45° refers to the plane of incident beam in the [110] direction projected onto the (100) face.)

mental data, are equivalent (at normal incidence) to comparing unshifted data with calculations using an inner potential of 6 eV. The earlier calculations [15,16] compared data in which the experimental energy scale was not "shifted" or referenced to some well defined level and used a 7.5 eV inner potential nearly equivalent to that found here.

In our comparisons to the shifted experimental data, peak positions agree most favorably at higher energies 150–200 eV. From 100 to 150 eV, an inner potential increased by ~2 eV would better match peak positions while from 50–100 eV in inner potential increased by ~3 eV is best. If we consider a contact potential difference (CPD) correction of about −2.5 eV [24], a non-static ($E > E_F$) inner potential

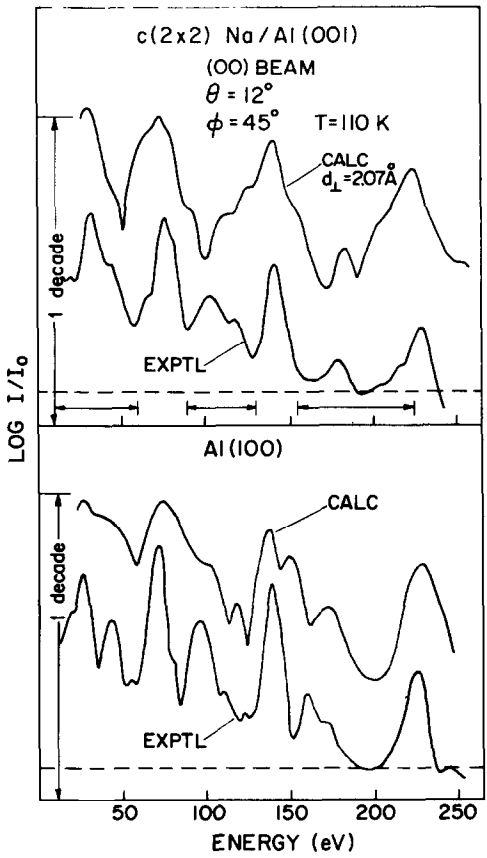

Fig. 7. Comparison of the (00) beam experimental results ($\theta = 12°$, $\phi = 45°$) for clean Al(100) with calculated spectra and Al(100)/Na–c(2×2). For the overlayer Na sits in the four-fold hollows. The experimental energy scale has been shifted by –6 eV. (Azimuthal angle of 45° refers to the plane of incident beam in the [110] direction projected onto the (100) face.)

of ~11.5, ~10.5 and ~8.5 eV in the ranges 50 to 100, 100 to 150, and 150 to 200 eV respectively would be needed to match the "uncorrected" experimental data. Such an estimate of the energy dependence of the inner potential is crude due to our lack of knowledge of the precise CPD correction as well as the small number of peak position considered here.

For the overlayer we observe similar peak displacements with energy. In fact, in fig. 3 for the $(\frac{1}{2}\,\frac{1}{2})$ beam the agreement at 1.96 Å is probably reduced due to the apparent displacement of the peaks below ~60 eV associated with an energy dependent inner potential (and our –6 eV shift of the experimental data to match peak positions at higher energies).

Some lack of agreement between theory and experiment occurs as we go to higher incident angles ($>7°$). In particular, for clean Al for $\theta = 12°$ as shown in fig. 7 the calculated peaks between 140–180 eV do not have the same shape as experiment. Spectra were also calculated for $\theta = 12° \pm 2°$, for $\phi = 43°$ and $47°$, for different inner potentials, for a different inner potential in the first Al layer, as well as for different bulk lattice spacings. We offer no resolution of this discrepancy. However, since the features observed at higher angles in Jona's Al(001) data [9] are nearly identical to those observed here, we believe this mismatch may be due to some wrong aspect of the current LEED model. (For Ni it has been found [25] that the treatment of exchange and correlation in the potential will affect calculated LEED spectra at higher energies – particularly at off normal incidence angles.)

Another feature of our results which deserves comment is that for the overlayer the best agreement between theory and experiment for the integral order beams occurs for a ~0.1 Å larger value of $d_\perp$ than for the fractional order beam. Whether this is real effect is not clear since only one fractional order beam has been considered. However such differences place an inherent uncertainty on establishing $d_\perp$ as well as the precise surface geometry of the Na/Al system. A distortion of the substrate layer immediately below the overlayer could conceivably lead one to select a larger $d_\perp$ for the Na overlayer atoms from the integral order beams. Calculations were done to test this hypothesis – the first Al layer was expanded and contracted by 0.1 Å and for each configuration $d_\perp$ for Na was varied as previously described. In either case the $(\frac{1}{2}\,\frac{1}{2})$ beam match was considerably worse than for the normal substrate, although the contracted substrate layer tended to shift the fractional order peak positions in a direction to favor a larger $d_\perp$. Substrate contractions smaller than ~0.1 Å as well as substrate distortions in a plane parallel to the surface might improve the fit and provide the same $d_\perp$ for both fractional and integral order beams. Since the latter distortions can not presently be modeled, this explanation remains untested.

5.2. Surface crystallography

A perpendicular distance of 2.05 ± 0.1 Å for the overlayer with the Na atom in a four-fold hollow corresponds to a bond length of 2.86 ± 0.07 Å (fig. 8). We compare this distance with the various bond radii of the components. A listing of bond radii is shown in table 1, where two values of the single bond covalent radii are listed: those of Pauling [26] (C–P) and a second set of Van Vechten and Phillips [27] (C–V). These two sets of covalent radii give bond lengths of 2.82 Å (C–P) and 2.84 Å (C–V) both within our experimental uncertainties. The use of a metallic radius for Al and a single bond covalent radius for Na gives bond lengths of 2.92 Å (C–V) or 3.00 Å (C–P).

These bond lengths can be compared with the case of c(2×2) Na on Ni(100) [5] where an experimental bond distance of 2.84 Å is found (corresponding to a perpendicular overlayer spacing of 2.23 Å for Na in a four-fold site). Use of single bond covalent radii for both Na and Ni gives a bond length of 2.71 Å (C–P) and 2.84 Å

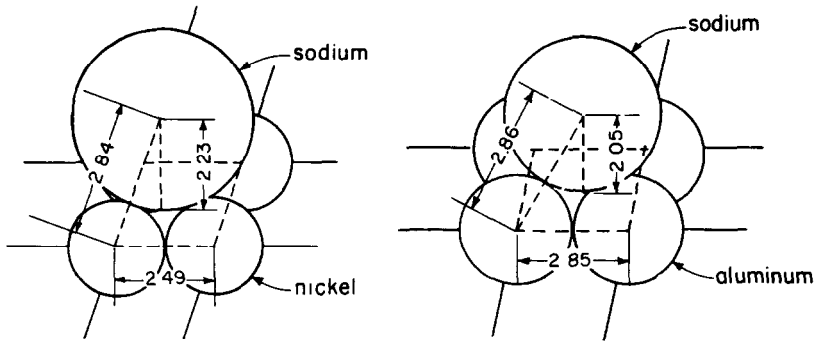

Fig. 8. Hard sphere model showing the local geometry and dimensions for Na on Ni(100) (left) and Na on Al(100) (right).

(C–V) while use of a metallic Ni radius gives a bond length of 2.80 Å (C–P) and 2.72 Å (C–V). It is thus possible to obtain reasonably good agreement for the determined bond lengths of both the Al/Na and the Ni/Na systems by using Van Vechten and Phillips single bond covalent radii for both substrate and overlayer.

6. Summary and conclusions

The structure of clean Al(100) and a c(2X2) Na overlayer has been determined. As found previously [15] no surface expansion or contraction occurs for the clean surface. However, a possible failure of the current Al LEED model to adequately describe the experimental results at higher energies and higher incident angles is observed. For the Na overlayer, it is found that Na resides in the four-fold hollow at a distance of 2.05 ± 0.1 Å from the surface. The corresponding Na–Al bond length for this location is 2.86 ± 0.07 Å. The bond lengths for Na/Al or Na/Ni c(2X2) structures are very much the same – consistent with the use of Van Vechten and Phillips [27] single band covalent radii for Na, Ni and Al. Alternatively, if we were to assume

Table 1
Bond radii of Na, Al and Ni

Notation		Radius (Å)		
		Na	Al	Ni
(C–P)	Single bond covalent [26]	1.57 Å	1.25 Å	1.14 Å
(C–V)	Single bond covalent [27]	1.49 Å	1.35 Å	1.35 Å
(M)	Metallic	1.85 Å	1.43 Å	1.23 Å

metallic substrate radii for Ni and Al, then the Na radius would depend upon the substrate.

A similar structural analysis of these same experimental results has been performed by Van Hove, Tong and Stoner [28] using not only a different theoretical computational method [29] but different input parameters. Within the stated accuracies both analyses agree – implying that structural determination at higher energies (> 50 eV) is much more critically dependent on the features of the trial geometry than the method of calculation or on the input parameters to the calculation.

Acknowledgements

Research support by National Science Foundation Grant DMR 71-01769 A02 and by the Advanced Research Project Agency through the Cornell Materials Science Center is acknowledged. One of us (J.E.D.) whishes to acknowledge many useful conversations with P.M. Marcus and D.W. Jepsen.

References

[1] F. Forstmann, W. Berndt and P. Buttner, Phys. Rev. Letters 30 (1973) 17.
[2] J.E. Demuth, D.W. Jepsen and P.M. Marcus, Phys. Rev. Letters 31 (1974) 540.
[3] J.E. Demuth, D.W. Jepsen and P.M. Marcus, Phys. Rev. Letters 32 (1974) 1182.
[4] M. Van Hove and S.Y. Tong, J. Vacuum Sci. Technol. 12 (1974) 230.
[5] A. Ignatiev, F. Jona, D.W. Jepsen and P.M. Marcus, J. Vacuum Sci. Technol. 12 (1975) 226.
[6] J.O. Porteus, Surface Sci. 41 (1974) 515.
[7] J.E. Demuth, D.W. Jepsen and P.M. Marcus, J. Phys. C8 (1975) 25.
[8] S. Anderson and J.B. Pendry, Solid State Commun. 16 (1975) 563.
[9] F. Jona, IBM J. Res. Develop. 14 (1970) 444.
[10] A. Ignatiev, A.V. Jones and T.N. Rhodin, Surface Sci. 30 (1972) 573.
[11] J.E. Demuth and T.N. Rhodin, Surface Sci. 42 (1974) 261; 45 (1974) 249; see J.E. Demuth, Ph.D. Thesis, Cornell Univ. (1973).
[12] D.T. Quinto and W.D. Robertson, Surface Sci. 27 (1971) 645.
[13] R.L. Gerlach and T.N. Rhodin, Surface Sci. 17 (1969) 32; 19 (1970) 403.
[14] J. Cross, J. Phys. D6 (1973) 622.
[15] D.W. Jepsen, P.M. Marcus and F. Jona, Phys. Rev. B5 (1972) 3933.
[16] C.B. Duke, N.O. Lipari and U. Landman, Phys. Rev. B8 (1973) 2454.
[17] V.L. Morruzzi, private communication.
[18] L. Hedin and B.I. Lundqvist, J. Phys. C4 (1971) 2064.
[19] From photoelectric measurements the work function for clean aluminum is determined to be ~3.9 eV; see R.Y. Koyama and N.V. Smith, Phys. Rev. B2 (1970) 3049.
[20] E.C. Snow, Phys. Rev. 172 (1968) 708.
[21] G.E. Laramore, Phys. Rev. B6 (1972) 1097.
[22] D.T. Quinto, B.W. Holland and W.D. Robertson, Surface Sci. 32 (1972) 139.
[23] B.I. Lundqvist, Phys. Status Solidi 32 (1969) 273. [See also, fig. 7 of D.W. Jepsen, P.M. Marcus and F. Jona, Phys. Rev. B12 (1973) 5523, for a plot of the energy dependence.]

[24] J.E. Demuth, D.W. Jepsen and P.M. Marcus, Surface Sci. 45 (1974) 733.
[25] S.Y. Tong, private communication.
[26] L.C. Pauling, The Nature of the Chemical Bond (Cornell Univ. Press, Ithaca, New York, 1940).
[27] J.A. Van Vechten and J.C. Phillips, Phys. Rev. B2 (1970) 2160;
J.A. Van Vechten, private communication.
[28] M. Van Hove, S.Y. Tong and A. Stoner, Surface Sci. 54 (1976)
[29] S.Y. Tong, in: Progress in Surface Science, Vol. 7, Part 2, Ed. S.G. Davison (Pergamon, Oxford, 1975).